spatiotemporal cats

# or, try herding 10 cats

*siminos/spatiotemp*, rev. 8223: last edit Predrag Cvitanović, 2022-02-23

Predrag Cvitanović, Han Liang, Sidney V. Williams,
Xuanqi Wang, Ibrahim Abu-hijeh, Andrew J. Fugett,
Rana Jafari, Li Han, Adrien K. Saremi and Boris Gutkin

March 1, 2022

## 4.1 Inverse iteration method

(Gábor Vattay, Sidney V. Williams and P. Cvitanović)

The 'inverse iteration method' for determining the periodic orbits of 2-dimensional repeller was introduced by G. Vattay as a ChaosBook.org exercise 4.1 *Inverse iteration method for a Hénon repeller* (see also the solution on page 187). The idea of the method is to

(1) Guess a lattice configuration $\phi_t^{(0)}$ that qualitatively looks like the desired lattice state. For that, you need a qualitative, symbolic dynamics description of system's admissible lattice states. You can get started by a peak at ChaosBook Table 18.1.

(2) Compare the 'stretched' field $\phi_t^{(0)}$ to its neighbors, using system's defining equation. For example, $\phi^3$ (or temporal Hénon) defining equation (3.23) is

$$-\phi_{t+1} + a\,\phi_t^2 - \phi_{t-1} = j_t\,.$$

Perhaps watch *What's "The Law"?* (4 min).

(3) Use the amount by which $\phi_t$ 'sticks out' in violation of the defining equations to obtain a better value $\phi_t^{(1)}$, for every lattice site $t$. Vattay does that by inverting the equation, determining $\phi_t^{(1)}$ from its neighbors

$$\phi_t^{(m+1)} = \sigma_t \frac{1}{\sqrt{a}} \left(1 + \phi_{t+1}^{(m)} + \phi_{t-1}^{(m)}\right)^{1/2} \tag{4.2}$$

where $\sigma_t$ is the sign of the target site field $\sigma_t = \phi_t/|\phi_t|$, prescribed in advance by specifying the desired Hénon symbol block

$$\sigma_t = 1 - 2\,m_t\,, \quad m_t \in \{0,1\}\,. \tag{4.3}$$

Perhaps watch *Inverse iteration method* (14:28 min).

(4) Wash and repeat, $\phi_t^{(m)} \to \phi_t^{(m+1)}$. Sidney starts the iteration by setting the initial guess lattice site fields to

$$\phi_t^{(0)} = \sigma_t/\sqrt{a}\,,$$

and then loops (4.2) through all lattice site fields to obtain $\phi_t^{(1)}$. When $|\phi_t^{(m+1)} - \phi_t^{(1)}|$ for all lattice states is smaller than a desired tolerance, the loop terminates, and the lattice state is found. An example of the resulting lattice states is given in figure 4.1.

The meat of the method is contained in these two loops:

```
for i in range(0,len(symbols)):
cycle[i]=signs[i]*np.sqrt(abs(1-np.roll(cycle,1)[i]-np.roll(cycle,-1)[i])/a)
for i in range(0,len(symbols)):
deviation[i]=np.roll(cycle,-1)[i]-(1-a*(cycle[i])**2-np.roll(cycle,1)[i])
```

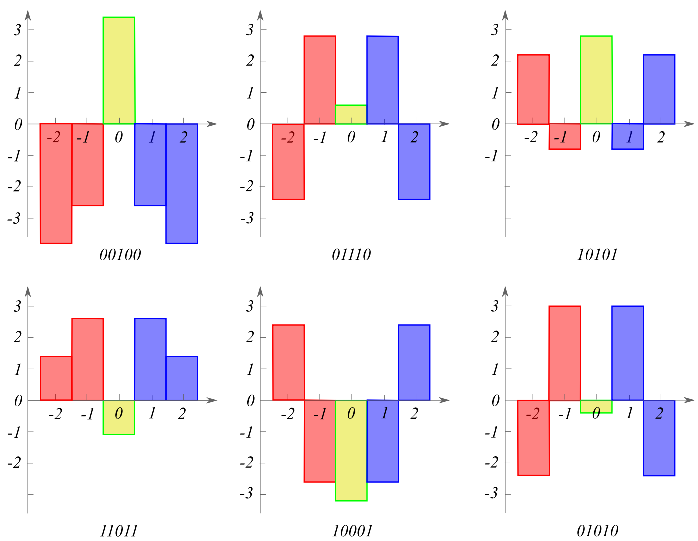


Figure 4.1: Temporal Hénon (3.23), $a = 6$: All period $n = 5$ prime lattice states $\overline{\phi_{-2}\phi_{-1}\boxed{\phi_0}\phi_1\phi_2|}$ of table 2.3. They are all reflection symmetric, with the fixed lattice field $\boxed{\phi_0}$ colored gold. The most striking feature is how far the $a = 6$ temporal Hénon is from the $0 \leftrightarrow 1$ symmetry: stretching close to $\overline{0}$ fixed point lattice state is much stronger than close to the almost marginal $\overline{1}$ fixed point lattice state. For a stretching parameter value $a$ slight lower than the critical value $a_h = 5.69931\cdots$, the lattice sites $\boxed{\phi_0}$ for $\overline{01110}$ and $\overline{01010}$ coalesce and vanish through an inverse bifurcation. As $a \to \infty$ we expect this symmetry to be restored.

The method applies to strongly coupled $\phi^3$ field theory in any spacetemporal dimension. For example, in 2 spacetime dimensions, the $m$th inverse iterate (4.2) compares the 'stretched' field $\phi_{nt}^{(0)}$ to its 4 neighbors,

$$\phi_{nt}^{(m+1)} = \sigma_{nt} \frac{1}{\sqrt{2a}} \left(2 + \phi_{n,t+1}^{(m)} + \phi_{n,t-1}^{(m)} + \phi_{n+1,t}^{(m)} + \phi_{n-1,t}^{(m)}\right)^{1/2} . \tag{4.4}$$

It is applied to each of the $LT$ lattice site fields $\{\phi_{nt}^{(m)}\}$ of a doubly periodic Bravais cell $[L\times T]_S$. Here $\sigma_{nt}$ is the sign of the target site field $\sigma_{nt} = \phi_{nt}/|\phi_{nt}|$, prescribed in advance by specifying the desired Hénon symbol block $\mathsf{M}$,

$$\sigma_{nt} = 1 - 2\, m_{nt} \,, \quad m_{nt} \in \{0, 1\} \,. \tag{4.5}$$

For the *temporal Hénon* 3-term recurrence (3.23), the system's state space Smale horseshoe is again generated by iterates of the region plotted in figure 4.2. So, positive field $\phi_{nt}$ value has $m_{nt} = 0$, negative field $\phi_{nt}$ value has $m_{nt} = 1$.

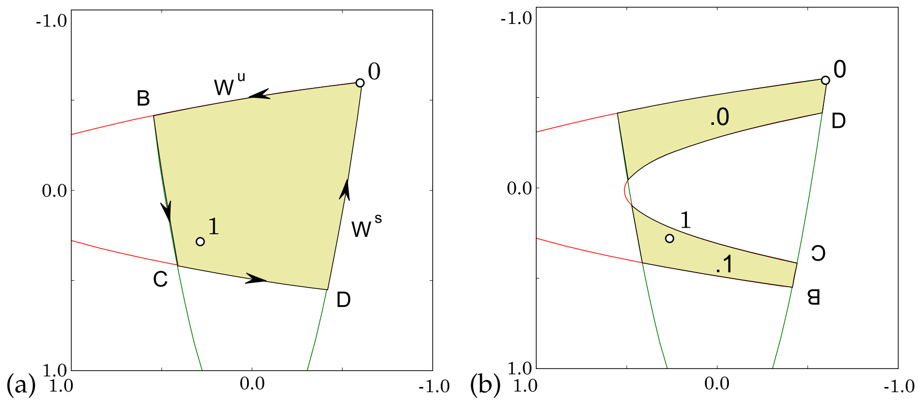


Figure 4.2: Temporal Hénon (2.2), (3.23) stable-unstable manifolds Smale horseshoe partition in the $(\phi_t, \phi_{t+1})$ plane for $a = 6$, $b = -1$: fixed point $\overline{0}$ with segments of its stable, unstable manifolds $W^s$, $W^u$, and fixed point $\overline{1}$. The most positive field value is the fixed point $\phi_0$. The other fixed point $\phi_1$ has negative stability multipliers, and is thus buried inside the horseshoe. (a) Their intersection bounds the region $\mathcal{M}_. = 0BCD$ which contains the non–wandering set $\Omega$. (b) The intersection of the forward image $f(\mathcal{M}_.)$ with $\mathcal{M}_.$ consists of two (future) strips $\mathcal{M}_{0.}$, $\mathcal{M}_{1.}$, with points $BCD$ brought closer to fixed point $\overline{0}$ by the stable manifold contraction. (The same as ChaosBook fig. 15.5, with $\phi_t = -x_t$.)

## 4.2 Shadow state method

*Have:* a partition of state space $\mathcal{M} = \mathcal{M}_A \cup \mathcal{M}_B \cup \cdots \cup \mathcal{M}_Z$, with regions $\mathcal{M}_m$ labelled by an $|\mathcal{A}|$-letter finite alphabet $\mathcal{A} = \{m\}$. The simplest example is temporal Hénon partition into two regions, named '0' and '1',

$$m_t \in \mathcal{A} = \{0, 1\}\,, \tag{4.6}$$

plotted in figure 4.2 (b). Prescribe a symbol block $\mathsf{M}$ over a finite Bravais cell of a $d$-dimensional lattice. A 1-dimensional example:

$$\mathsf{M} = (m_0, \cdots, m_{n-1})\,. \tag{4.7}$$

*Want:* the lattice state $\Phi_\mathsf{M}$ whose lattice site fields $\phi_t$ lie in state space domains $\phi_t \in \mathcal{M}_m$, as prescribed by the given symbol block $\mathsf{M}$. A 1-dimensional example:

$$\Phi_\mathsf{M} = (\phi_0, \cdots, \phi_{n-1})\,, \quad \phi_t \in \mathcal{M}_m\,, \tag{4.8}$$

By *lattice state* $\Phi$ we mean a point in the $n$-dimensional state space that is a solution of the defining Euler-Lagrange equation. For the temporal Hénon example, that equation is the 3-term recurrence (3.23),

$$-\,\phi_{t+1} + a\,\phi_t^2 - \phi_{t-1} = j_t\,, \quad j_t = 1\,, \tag{4.9}$$

with all $a = 6$ period-5 lattice states plotted in figure 4.1.

**Shadow state method.** Construct a *shadow state* $\overline{\Phi}_{\mathsf{M}}$ and the *forcing* $j(\mathsf{M})_t$ such that the site-by-site deviation

$$\varphi_t = \phi_t - \overline{\phi}_t \tag{4.10}$$

is small. Determine the desired lattice state $\Phi_{\mathsf{M}}$ as the neighboring $|\Phi_{\mathsf{M}} - \overline{\Phi}_{\mathsf{M}}|$ fixed point of the M-forced Euler-Lagrange equation.
*Desideratum:* Plot the first, $n = 6$ temporal Hénon asymmetric lattice state $\Phi_{\mathsf{M}}$ and shadow state $\overline{\Phi}_{\mathsf{M}}$, to illustrated the idea.

First, determine the fixed points (solutions with a constant field on all lattice sites) $\phi_t = \overline{\phi}_m$. For temporal Hénon there are two, $\overline{\phi}_0$ and $\overline{\phi}_1$ (see figure 4.2), labeled by the alphabet (4.6).

Next, construct the simplest configuration from $|\mathcal{A}|$ fields $\overline{\phi}_m$, each field in the domain of state space prescribed by the symbol block M. In the shadow state method, we pick a fixed point $\overline{\phi}_m$ in each domain as domain's representative $\overline{\phi}_m \in \mathcal{M}_m$. For the temporal Hénon example, the fixed-points *shadow state* is:

$$\overline{\Phi}_{\mathsf{M}} = (\overline{\phi}_0, \cdots, \overline{\phi}_{n-1}) \,, \qquad \text{where } \overline{\phi}_t = \begin{cases} \overline{\phi}_0 \text{ if } m_t = 0 \\ \overline{\phi}_1 \text{ if } m_t = 1. \end{cases} \tag{4.11}$$

In general, the shadow state $\overline{\Phi}_{\mathsf{M}}$ does not satisfy the Euler-Lagrange equation (4.9), violating it by amount $\overline{j}(\mathsf{M})_t$

$$-\,\overline{\phi}_{t+1} + a\,\overline{\phi}_t^2 - \overline{\phi}_{t-1} = 1 - \overline{j}(\mathsf{M})_t \,, \tag{4.12}$$

where the forcing $\overline{j}(\mathsf{M})_t$ depends on $\overline{\phi}_t$ and its neighbors. For the temporal Hénon example, it takes the values tabulated in table 4.1.

Subtract (4.12) from (4.9) to obtain the 3-term recurrence for $\varphi_t = \phi_t - \overline{\phi}_t$, the deviations (4.10) from the shadow state,

$$-\varphi_{t+1} + a\,(\phi_t^2 - \overline{\phi}_t^2) - \varphi_{t-1} = \overline{j}(\mathsf{M})_t \,.$$

Substituting $\phi_t^2 = (\varphi_t + \overline{\phi}_t)^2$ , we obtain the *exact*

M**-forced 3-term recurrence** for the deviations $\varphi_t$ from the shadow state lattice configuration $\overline{\Phi}_{\mathsf{M}}$,

$$-\varphi_{t+1} + a\,(\varphi_t + \overline{\phi}_t)^2 - \varphi_{t-1} \quad = \quad j(\mathsf{M})_t \,, \tag{4.13}$$

where $j(\mathsf{M})_t = \overline{j}(\mathsf{M})_t - a\,\overline{\phi}_t^2$, one such recurrence for each admissible symbol block M. [1]

| $m_{t-1}m_tm_{t+1}$ | $\overline{j}(\mathsf{M})_t$ | | |
|---|---|---|---|
| 0 0 0 | 0 | | |
| 0 0 1 = 1 0 0 | -A | = | $\overline{\phi}_1 - \overline{\phi}_0$ |
| 0 1 0 | -B | = | $a(\overline{\phi}_1^2 - \overline{\phi}_0^2)$ |
| 1 0 1 | B | = | $a(\overline{\phi}_0^2 - \overline{\phi}_1^2)$ |
| 1 1 0 = 0 1 1 | A | = | $\overline{\phi}_0 - \overline{\phi}_1$ |
| 1 1 1 | 0 | | |

Table 4.1: Temporal Hénon fixed-points shadow state $\overline{\Phi}_\mathsf{M}$ forcing $\overline{j}(\mathsf{M})_t$ depends on 3 lattice sites $m_{t-1}m_tm_{t+1}$, and takes values $(0, \pm A, \pm B)$. If period-2 or longer lattice states are utilized as shadows, more neighbors contribute.

**Vattay inverse iteration** (4.2) is now

$$\varphi_t^{(m+1)} = -\overline{\phi}_t + \sigma_t \frac{1}{\sqrt{a}} \left( j(\mathsf{M})_t + \varphi_{t+1}^{(m)} + \varphi_{t-1}^{(m)} \right)^{1/2} , \tag{4.14}$$

and that should converge like a ton of rocks.

Perhaps watch *Shadow state conspiracy* (35:26 min)

**Summary**

1. M-forced 3-term recurrence (4.13) is *exact*. It is superior to the original recurrence as it has built-in symbolic dynamics. The deviations $\varphi_t = \phi_t - \overline{\phi}_t$ should be small, and the topological guess based on M-forcing should be robust. The recurrence can be solved by any method you like.
2. $\phi^4$ field theory works the same, with the M-forced 3-term recurrence for the deviations $\varphi_t$ now built from approximate 3-field values $(\overline{\phi}_L, \overline{\phi}_C = 0, \overline{\phi}_R)$. If using Vattay (4.14), the Hénon sign $\sigma_t$ needs to be rethought.
3. Implement M-forced 3-term recurrence for symmetric states boundary conditions.
4. Generalization to higher spatiotemporal dimensions is immediate (see, for example, the 2-dimensional Vattay iteration (4.4)).
5. As one determines larger and larger Bravais cell lattice states, on can use the already computed ones instead of the initial $(\overline{\phi}_0, \overline{\phi}_1)$ to get increasingly better $M$-forced shadowing.
6. The boring forcing term $j_t = 1$ on RHS of the temporal Hénon recurrence (4.9) has been replaced by a non-trivial forcing $j(\mathsf{M})_t$ in (4.13), as hoped for.
7. This is not the Biham-Wentzel method: it's based on exact Euler-Lagrange equations, there are no artificially inverted potentials, as we are not constructing an attractor; all our solutins are and should be unstable.

8. The Newton method requires evaluation of the orbit Jacobian matrix $\mathcal{J}$. As we have only *translated* field values $\phi_t \to \varphi_t$, $\mathcal{J}$ is the same as for the original 3-term recurrence. For large lattice states variational methods discussed below should be far superior to simple Newton.

9. Have a look at Fourier transform of (4.13). Anything gained in Fourier space? Remember, we have not quotiented translation symmetry, we are still computing $n$ lattice states on the spatiotemporal lattice.

[2] A. Brown, "Equations for periodic solutions of a logistic difference equation", J. Austral. Math. Soc. Ser. B **23**, 78–94 (1981).

[3] P. Cvitanović and Y. Lan, Turbulent fields and their recurrences, in Correlations and Fluctuations in QCD : Proceedings of 10. International Workshop on Multiparticle Production, edited by N. Antoniou (2003), pp. 313–325.

[4] C. Dong, "Topological classification of periodic orbits in Lorenz system", Chin. Phys. B **27**, 080501 (2018).

[5] C. Dong, "Topological classification of periodic orbits in the Yang-Chen system", Europhys. Lett. **123**, 20005 (2018).

[6] C. Dong and Y. Lan, "A variational approach to connecting orbits in nonlinear dynamical systems", Phys. Lett. A **378**, 705–712 (2014).

[7] C. Dong and Y. Lan, "Organization of spatially periodic solutions of the steady Kuramoto-Sivashinsky equation", Commun. Nonlinear Sci. Numer. Simul. **19**, 2140–2153 (2014).

[8] C. Dong, H. Liu, and H. Li, "Unstable periodic orbits analysis in the generalized Lorenz-type system", J. Stat. Mech. **2020**, 073211 (2020).

[9] A. Endler and J. A. C. Gallas, "Period four stability and multistability domains for the Hénon map", Physica A **295**, 285–290 (2001).

[10] A. Endler and J. A. C. Gallas, "Arithmetical signatures of the dynamics of the Hénon map", Phys. Rev. E **65**, 036231 (2002).

[11] A. Endler and J. A. C. Gallas, "Conjugacy classes and chiral doublets in the Hénon Hamiltonian repeller", Phys. Lett. A **356**, 1–7 (2006).

[12] A. Endler and J. A. C. Gallas, "Reductions and simplifications of orbital sums in a Hamiltonian repeller", Phys. Lett. A **352**, 124–128 (2006).

[13] A. Endler and J. A. C. Gallas, "Reductions and simplifications of orbital sums in a Hamiltonian repeller", Phys. Lett. A **352**, 124–128 (2006).

[14] J. A. C. Gallas, "Equivalence among orbital equations of polynomial maps", Int. J. Modern Phys. C **29**, 1850082 (2018).

[15] J. A. C. Gallas, "Orbital carriers and inheritance in discrete-time quadratic dynamics", Int. J. Modern Phys. C **31**, 2050100 (2020).

[16] J. A. C. Gallas, "Preperiodicity and systematic extraction of periodic orbits of the quadratic map", Int. J. Modern Phys. C **31**, 2050174 (2020).

[17] A. Gao, J. Xie, and Y. Lan, "Accelerating cycle expansions by dynamical conjugacy", J. Stat. Phys. **146**, 56–66 (2012).

[18] F. Gao, H. Gao, Z. Li, H. Tong, and J.-J. Lee, "Detecting unstable periodic orbits of nonlinear mappings by a novel quantum-behaved particle swarm optimization non-Lyapunov way", Chaos Solit. Fract. **42**, 2450–2463 (2009).

[19] M. N. Gudorf, Spatiotemporal Tiling of the Kuramoto-Sivashinsky Equation, PhD thesis (School of Physics, Georgia Inst. of Technology, Atlanta, 2020).

[20] M. N. Gudorf, Orbithunter: Framework for Nonlinear Dynamics and Chaos, tech. rep. (School of Physics, Georgia Tech, 2021).

[21] Y. Lan, Dynamical Systems Approach to $1-d$ Spatiotemporal Chaos – A Cyclist's View, PhD thesis (School of Physics, Georgia Inst. of Technology, Atlanta, 2004).

[22] Y. Lan, C. Chandre, and P. Cvitanović, "Variational method for locating invariant tori", Phys. Rev. E **74**, 046206 (2006).

[23] Y. Lan and P. Cvitanović, "Variational method for finding periodic orbits in a general flow", Phys. Rev. E **69**, 016217 (2004).

[24] Y. Lan and P. Cvitanović, "Unstable recurrent patterns in Kuramoto-Sivashinsky dynamics", Phys. Rev. E **78**, 026208 (2008).

[25] H. Liu, C. Dong, Q. Jie, and H. Li, "Topological classification of periodic orbits in the generalized Lorenz-type system with diverse symbolic dynamics", Chaos, Solitons & Fractals **154**, 111686 (2022).

[26] W. H. Press, B. P. Flannery, S. A. Teukolsky, and W. T. Vetterling, *Numerical Recipes*, 3rd ed. (Cambridge Univ. Press, Cambridge UK, 2007).

[27] J. Stephenson and D. T. Ridgway, "Formulae for cycles in the Mandelbrot set II", Physica A **190**, 104–116 (1992).

[28] D. Wang and Y. Lan, A reduced variational approach for searching cycles in high-dimensional systems, 2022.

[29] D. Wang, P. Wang, and Y. Lan, "Accelerated variational approach for searching cycles", Phys. Rev. E **98**, 042204 (2018).

[30] X. Zhou, W. Ren, and E, W., "Adaptive minimum action method for the study of rare events", J. Chem. Phys. **128**, 104111 (2008).